Journal of Oral Health and Biosciences 34(2):40 ～ 52, 2022

Original Article

Dendritic Cells Directly Recognize Nickel Ions as an Antigen during the Development of Nickel Allergy

Lipei LIU[1)], Megumi WATANABE[2)], Norikazu MINAMI[1)], Mohammad Fadyl YUNIZAR[1)], Tetsuo ICHIKAWA[1)]

Keywords：Metal allergy, Nickel ions, Phagocytosis, Dendritic cell migration

Abstract：Metal hypersensitivity, a disorder of the immune system, typically manifests as contact hypersensitivity to metals during daily contact. The molecular mechanism whereby metals enter the body and cause allergic disorders remains elusive. It is thought that eluted metal ions are captured by dendritic cells (DCs) and transferred to the draining lymph nodes to activate T cells. Here, for the first time, we used a metal indicator Newport Green to locate the most common allergenic metal, nickel (Ni) ions, captured by DCs and transferred to lymph nodes. Capturing Ni ions did not affect the activity of DCs. Ni ions entered DCs and showed positive staining in keratinocytes. A time varied quantitative analysis demonstrated that at 1 h, a small amount of Ni ions was observed in the epidermal sheet. After 6 h, the number of Ni ions that entered the epidermal sheet reached a peak and remained constant for a few days and were gradually emitted 48 h later. In the cervical lymph nodes of mice, accumulation of Ni ions reached a peak within 24 h and then gradually decreased. The findings of this study will contribute to the development of effective diagnoses and treatment methods for patients allergic to Ni.

Introduction

Metal allergy is a public health concern that has a major impact on individuals, society, and the economy, bringing a heavy physical, mental, and economic burden to patients. Nickel (Ni) is the most common cause of contact allergy in the general population and is the most common allergen detected by patch testing in patients with suspected allergic contact dermatitis (ACD)[1)]. Ni ACD is a typical type IV hypersensitivity reaction. Ni exposure primarily arises from daily supplies, such as jewelry and clothing decoration, metal tools, medical equipment such as orthopedic and orthodontic implants, and cosmetics. The typical clinical feature of ACD caused by Ni is eczema dermatitis, which occurs on the skin area that is in direct contact with metals. Symptoms include lichenoid dermatitis, annular granuloma, vitiligo-like lesions, and systemic contact dermatitis[1)].

During sensitization and elicitation phases of Ni allergy reactions, both innate and adaptive immune systems are activated in a complex manner and whose mechanism has not been fully elucidated[2)]. Metal attachment to skin or mucous membranes and body invasion is the first step in inducing metal allergies. Therefore, it is believed that the metal must be ionized and eluted. Studies show that keratinocytes on the surface of the skin and mucous membranes first react with metals eluted by sweat or saliva and subsequently act on surrounding immune cells through cytokines such as thymic stromal lymphopoietin to form a pathological microenvironment. There is no information regarding how cells perceive and capture Ni ions. A study showed that Ni directly binds to the human leukocyte antigen without peptide

[1)] Department of Prosthodontics & Oral Rehabilitation, Tokushima University, Graduate School of Bio-medical Sciences
[2)] Tokushima University Hospital

mediation[3], whereas another study highlighted that Ni ions penetrate the skin and directly interact with Toll-like receptor 4 on dendritic cells (DCs), resulting in the stimulation of the IKK2-nuclear factor-κB cascade to induce the occurrence of allergies[4]. Activated DCs upregulate costimulatory molecules and migrate to local lymph nodes, where Ni is present in naive T cells via major histocompatibility complex (MHC) II molecules. Subsequently, allergen-specific T cells and memory T cells proliferate and migrate into the blood and skin, leading to sensitization[5, 6]. In the elicitation phase, re-entry of Ni ions can rapidly trigger allergic dermatitis[7]. In addition, Hirai et al. showed that metal nanoparticles, especially those sized 10 nm or smaller, are new potential causes of metal allergy and can be transported to draining lymph nodes[8].

The primary barrier to Ni penetration is the stratum corneum[9]. Existing literature shows that Ni can penetrate the stratum corneum in three ways: transcellular, intercellular, or appendages[10]. Water-soluble Ni salts are mostly deposited on the outside of the stratum corneum[11]. Ni reacts with weak organic acids to produce different degrees of lipophilic Ni soap, which can penetrate the skin through the intercellular route[10, 12]. Ni can strongly chelate histidine-rich filaggrin proteins, which slows down penetration through the stratum corneum[13]. Ni reacts with sweat to form divalent Ni ions and penetrates the skin via the three methods mentioned above[11]. However, studies have shown that trivalent Ni ions, rather than divalent Ni ions, are the main immunogenic forms of Ni allergy[14]. In addition, penetration is also determined by skin thickness, temperature, humidity, pH, hair follicle density, and blood flow[15, 16].

Newport Green™ DCF is a metal indicator with moderate zinc (Zn) binding affinity. It demonstrates a positive effect on transition metals including Zn, Mn, Fe, Co, Cu (I), Cu (II), Ni, and Cd. Thus, Newport Green™ DCF was adapted as a probe for this study. The aim of this study was to further elucidate the initial mechanism of metal allergy, i.e., the extent to which invading Ni ions are carried in DCs, how they react with keratinocytes, and how they are transmitted.

By studying the mechanism of Ni allergy, we hope to contribute to the development of effective diagnosis and treatment methods for patients allergic to Ni.

Materials and Methods

Mice

Female C57BL/6J mice (8-week-old) were purchased from Charles River Laboratories, Inc. (Kanagawa, Japan) and maintained under specific pathogen-free conditions at Tokushima University. All experimental procedures were approved by IACUC (No. T2019-51) and Institute for Genome Research (No.30-46) of Tokushima University.

Bone marrow-derived DC (BMDC) isolation and culture

Femurs and tibias were harvested from female C57BL/6J wild-type mice. The muscle and tissue of the bones were mechanically debrided and the ends of the bones were cut. A 23 G needle was used to flush out the bone marrow into a dish of PBS on ice. After filtering through a 40 μm cell sieve, red blood cells were lysed. Cells were centrifuged, quantified and resuspended in RPMI1640 (nacalai tesque, Kyoto, Japan) containing GM-CSF (10 ng/ml), IL-4 (1 ng/ml), 10 %FBS (biowest, Nuaillé, France), 1 % penicillin/streptomycin/amphotericin B (nacalai tesque, Kyoto, Japan) in 8 well chamber slide (Thermo Scientific Nunc Lab-Tek) or 35 mm dish. On day 2, 4, 6, media was half removed and centrifuged, those loosely adherent cells contained in the removed media were added back to dishes with fresh media. BMDCs were treated with 25 μM $NiCl_2$ for 0, 1, 3, 6, 12, 24, 48, 72 h before subsequent analysis of immunofluorescence staining and flow cytometry.

Induction of Ni Allergy

Ni allergy was induced on mouse ears as described previously[17-19]. Briefly, 25 μl 1 mM $NiCl_2$ (Wako Pure Chemical Corporation) with 25 μl Freund's incomplete adjuvant (IFA) was intraperitoneally injected into C57BL/6J for initial immunization, followed by a intradermal injection of 10 μl 0.2 mM $NiCl_2$ with 10 μl complete adjuvant (CFA) in the ear skin as a second challenge 2 weeks later. The cervical lymph nodes were harvested 0, 24, 48 and 72 h after Ni allergy induction for immunofluorescence staining and flow cytometry analysis.

Epidermal sheet preparation

Epidermal sheets were prepared using a modification of previously-reported method[20, 21]. In short, the ears were peeled in half and floated dermis-side down on cold ammonium thiocyanate. After incubation at 37 ℃ for 13 minutes, the epidermal sheets were peeled off with tweezers, after washed with PBS and fixed with cold acetone, they were used for immunofluorescence staining.

Immunofluorescence microscopy

Frozen sections (10 μm) of cervical lymph nodes were fixed with cold acetone for 10 minutes. After washing with PBS and blocking with 5 % goat serum for 30 minutes, a 1:300 dilution of Newport Green™ DCF indicator (Thermo Fisher Scientific) and PE anti-mouse I-A/I-E (BioLegend) were applied to the sections and incubated overnight at 4 ℃ in dark. Cell nuclei were stained with DAPI solution (0.1 μg/ml; Cell Signaling Technology, Danvers, MA, USA). Keyence all-in-one fluorescence-microscope BZ-X800 (magnification, × 100;

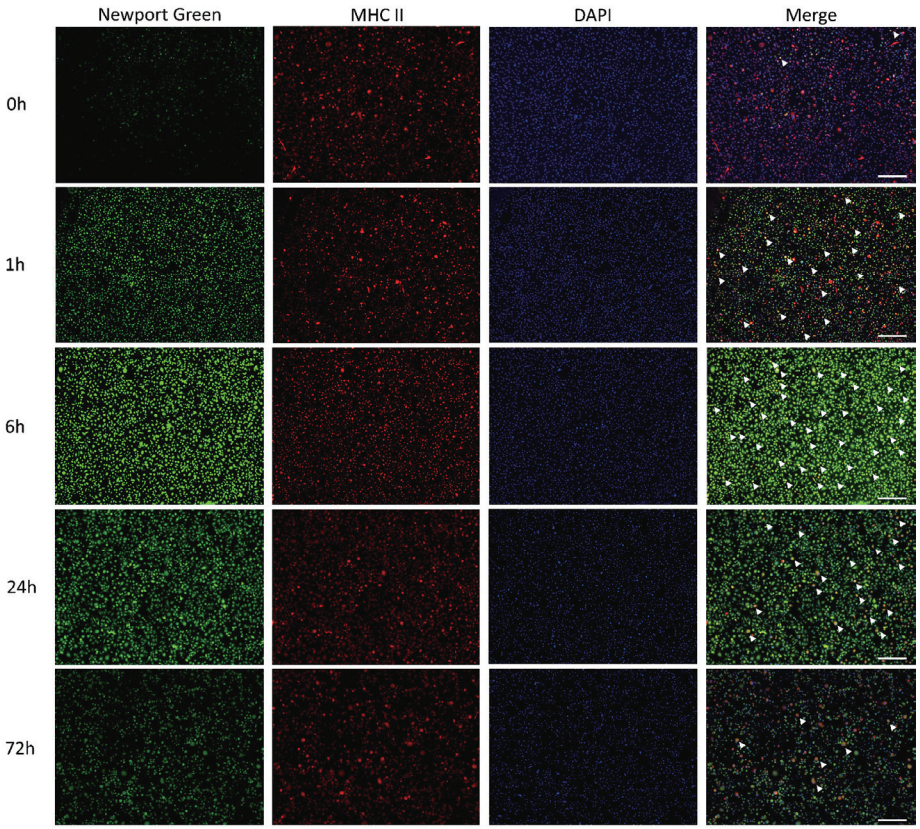

Fig. 1 Immunofluorescence images of Ni-stimulated BMDCs.
Immunofluorescence images of Newport Green and MHC II expression in cultured BMDCs after 25 μM $NiCl_2$ stimulation over time. The yellow color (partially indicated by arrow heads) in merged photos represents the DCs that captured Ni ions. The number of double-positive cells showed a peak at 6 h group after Ni stimulation. Magnification, × 100. Scale bar, 200 μm.

× 200; × 400; × 1000; KEYENCE CORPORATION, Tokyo, Japan) was used for taking immunofluorescence images. BZ-X800 Analyzer software was adapted for the extraction and quantification of Newport Green-positive areas.

Flow cytometry

1×10^6 cells of single-cell suspensions of mouse cervical lymph nodes as well as BMDCs were stained with Newport Green and PE anti-mouse I-A/I-E according to the recommended concentration. Cells were analyzed on BD FACSVerse™ (BDBiosciences, San Jose, CA, USA).

Results

Ni ion was captured by BMDCs

In an *in vitro* experiment, we isolated and cultured DCs from the bone marrow of mice. Thereafter, they were stimulated with 25 μM $NiCl_2$ at different time periods. The double staining results of Newport Green, which can recognize Ni and MHC II, showed that BMDCs that were not stimulated by Ni were negatively stained for Newport Green. The double staining of Newport Green and MHC II is shown in yellow in the merged photos (Fig. 1), which indicates the position of BMDCs that captured Ni ions. One hour after the addition of Ni, Newport Green-positive staining appeared in BMDCs. The intensity of the stain increased 3 h after Ni stimulation; the strongest positive staining was observed at 6 h, and then gradually decreased at 12, 24, 48, and 72 h. The staining at 72 h was marginally stronger than that at the start of Ni stimulation (Fig. 1 and Fig. S1). In addition, double-positive staining of granular particles in the cell matrix, which indicates the position of Ni ions, was observed after 3 h of Ni stimulation in Ni-stimulated BMDCs at 1000 × magnification (Fig. 2).

According to fluorescence cell count results using BZ-X800 Analyzer software, the extraction area of Newport Green-positive cells reached a peak at 6 h after Ni stimulation, and decreased gradually thereafter (Fig. 3A). BMDCs were subsequently collected and fluorescence-activated cell sorting (FACS) analysis was performed. The results were consistent with those of immunofluorescence staining; the number of Newport Green-positive cells increased after Ni stimulation compared to the control group, which was not stimulated with

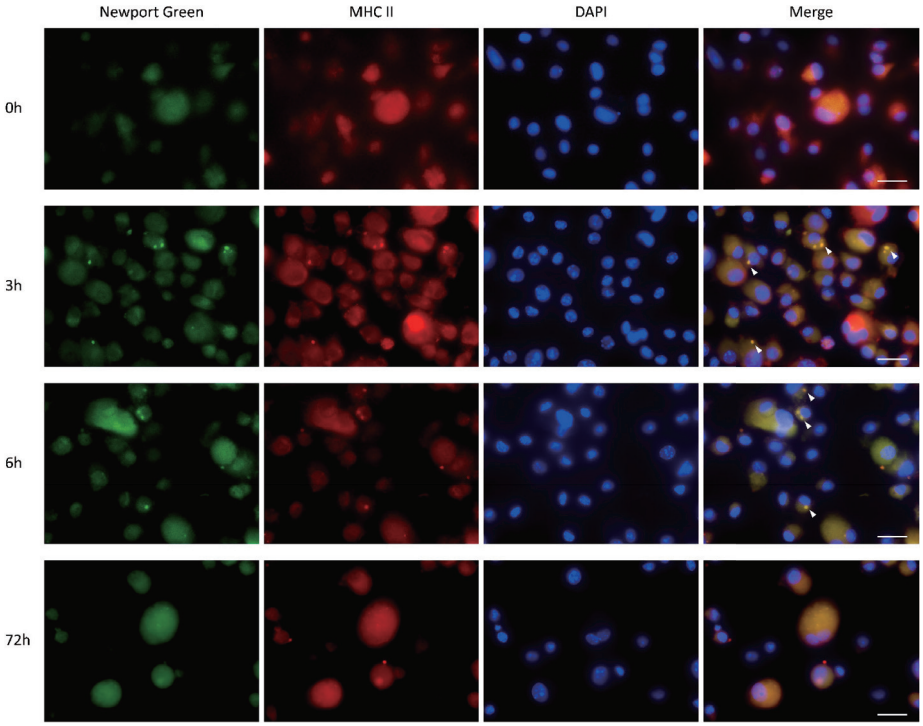

Fig. 2 Immunofluorescence images of of Ni-stimulated BMDCs in large magnification.
Immunofluorescence images of Newport Green and MHC II expression in cultured BMDCs after 25 μM $NiCl_2$ stimulation over time. Arrow heads indicate the double-positive granular particles of Ni ions. Magnification, × 1000. Scale bar, 20 μm.

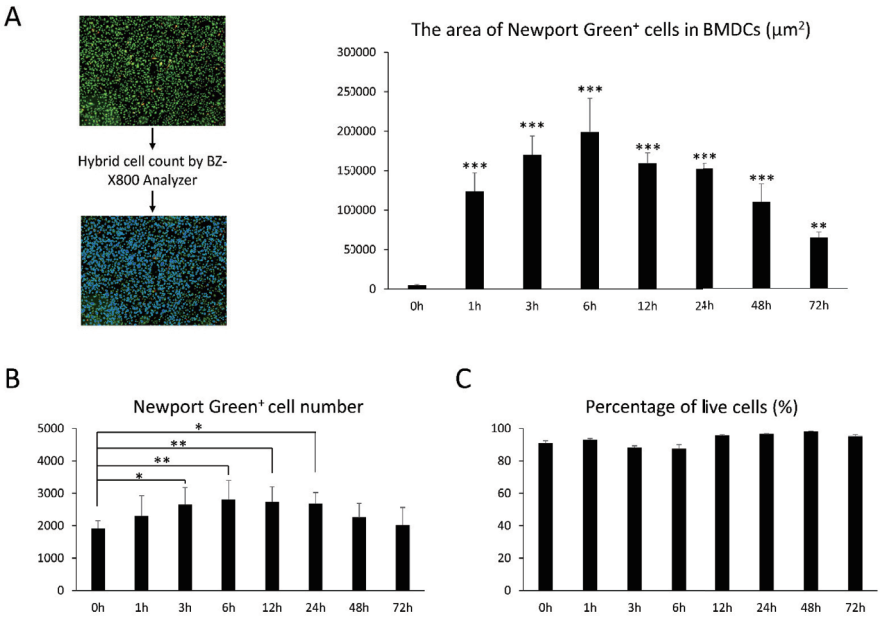

Fig. 3 The population analysis of BMDCs.
(A) The left panel gives the example of fluorescence hybrid cell count by BZ-X800 Analyzer software. After analysis, the Newport Green-positive area will be extracted as blue color. The right panel shows the quantification result of the area of Newport Green-positive cells in the BMDCs after Ni stimulation over time. Data are shown as mean ± SD of at least 4 images/group.
(B) The population of Newport Green-positive cells in BMDCs was analyzed by flow cytometry.
(C) The population of live cells in BMDCs was analyzed by flow cytometry through Propidium Iodide staining.
*p<0.05, **p<0.01, ***p<0.001, compared to 0 h group. One-Way ANOVA with LSD.

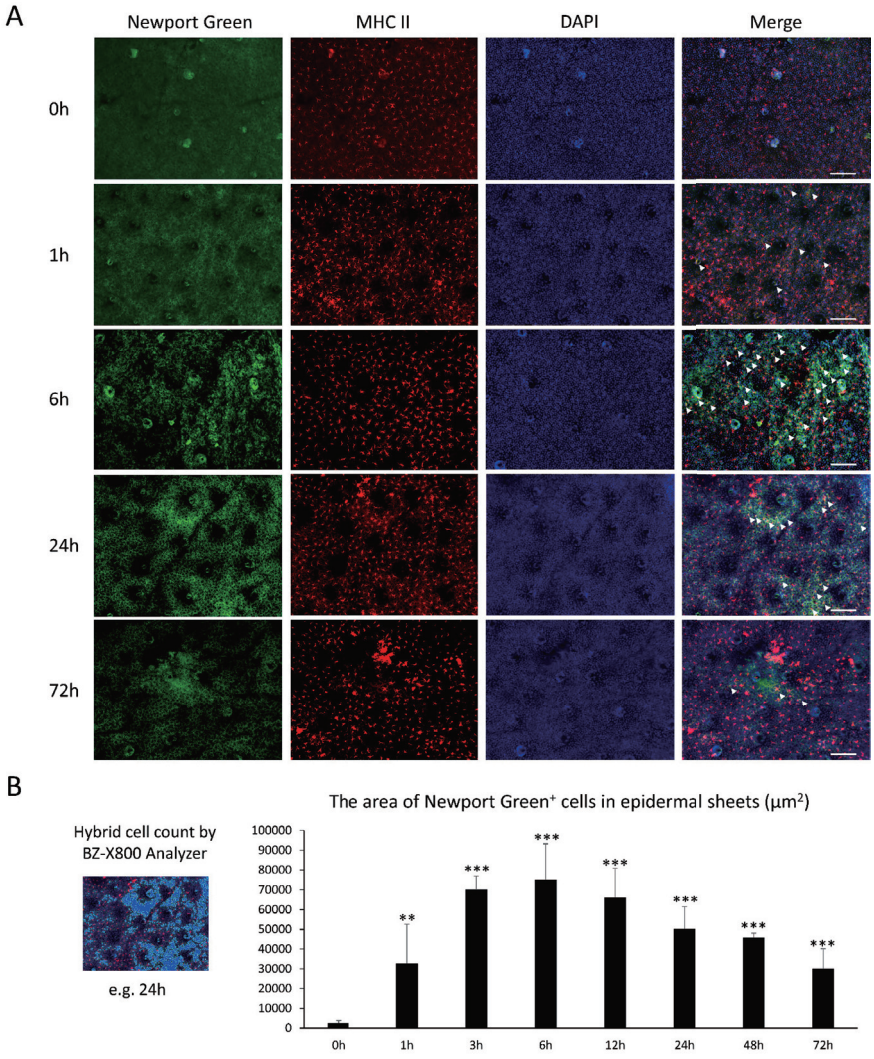

Fig. 4 Immunofluorescence images of of Ni allergy-induced mouse epidermal sheets.
(A) Immunofluorescence images of Newport Green and MHC II expression in epidermal sheets after Ni allergy induction over time. The yellow color (partially indicated by arrow heads) in merged photos represents the DCs that captured Ni ions. Magnification, × 200. Scale bar, 100 μm.
(B) The left panel shows the example of 24 h group image after fluorescence hybrid cell count by BZ-X800 Analyzer software. The blue area indicates the Newport Green-positive area after extraction. The right panel shows the quantification result of the area of Newport Green-positive cells in the Ni allergy-induced epidermal sheets over time. Data are shown as mean ± SD of at least 3 images/group. **p<0.01, ***p<0.001, compared to 0 h group. One-Way ANOVA with LSD.

Ni and reached its peak at 6 h (Fig. 3B).

To confirm cell viability, propidium iodide staining was used. FACS results showed that the cells stimulated with 25 μM $NiCl_2$ and the unstimulated control group showed no difference in the number of viable cells, which reached 90 % of the total cell number (Fig. 3C). Therefore, the concentration of Ni^{2+} did not affect cell viability, nor did it cause additional effects.

Ni ion was captured by epidermal DCs

To further confirm whether Ni was captured by DCs in *in vivo* experiments, we used a Ni allergy mouse model. At different time points after the Ni allergy induction, ear tissue of the mouse was collected, and epidermal sheets were peeled off. Newport Green and MHC II were used to stain epidermal sheets.

The results demonstrated that epidermal DCs (or Langerhans cells) could capture Ni ions; similarly, Newport Green-positive staining was also observed in keratinocytes. Immunofluorescence staining showed that the epidermal sheet only showed weak and inconspicuous staining 1 h after Ni allergy induction (Fig. 4A). However, 3 h after Ni

allergy induction, double-positive stained spots were evident, showing the location of DCs that captured Ni ions (Fig. S4 and Fig. 4A). BZ-X800 Analyzer software showed that the extraction area of Newport Green-positive cells in Ni allergy-induced epidermal sheets gradually increased and reached a peak at 6 h, which subsequently decreased (Fig. 4B).

Ni ions were transmitted to lymph nodes by epidermal DCs

DCs located in the skin migrate through lymph vessels to lymph nodes and present antigens to trigger an immune response to pathogens. To confirm whether epidermal DCs transfer Ni ions to lymph nodes, at 6, 12, 24, 48 and 72 h after Ni allergy induction, cervical lymph nodes were collected from each group and the control group for immunofluorescence staining of frozen sections and FACS analysis of single cell suspensions.

For immunofluorescence staining of frozen sections, no Newport Green-positive staining was observed in the control group. However, 6 h after Ni allergy induction, a small amount of Newport Green-positive staining appeared in lymph node sections. The sites of double-positive staining gradually increased in the 12, 24 and 48 h groups and decreased in the 72 h group (Fig. 5A). For the fluorescence cell count using the BZ-X800 Analyzer software, Newport Green-positive areas were extracted in the specified lymph node area. The area percentage of the Newport Green-positive cells in lymph nodes increased and showed a peak in the 24 h group (Fig. 5B).

Representative time points of 0, 24, 48 and 72 h were selected, lymph nodes of five mice in each group were collected, and FACS analysis was performed (Fig. 6A). The results showed that 24 h after Ni allergy induction, the number of Newport Green-positive cells reached a peak and gradually decreased over time (Fig. 6C). Additionally, the number of double-positive cells for Newport Green and MHC II was less than that of cells positive for Newport Green only (Fig. 6B). This indicated that in addition to DCs, there were other cells that have also captured or transferred Ni ions.

Discussion

Humans are inevitably exposed to Ni as it is ubiquitous in our environment. Metal objects, household products, and cosmetics can cause local skin Ni exposure, and food, water, surgical implants, and dental materials can cause systemic exposure. Ni causes allergies when deposited on the skin and when it penetrates the skin.

A deposition experiment performed by Julander et al. using Ni-containing coins showed that Ni is deposited on the skin at high doses; the total amount of Ni released from coins immersed in artificial sweat increases over time, and the Ni release rate is initially quick, but subsequently slows down gradually[22]. Erfani et al. confirmed that short-term and frequent contact with Ni-containing materials can lead to the accumulation of high doses of Ni on the skin. However, the amount of Ni released by repeated immersion in artificial sweat is lower than that of Ni released in touch and wipe tests[23]. Fournier et al. also confirmed that the friction inherent in daily use primarily assists Ni transfer to hands[24]. It was thought that skin deposition of Ni requires long-term contact between the metal and the skin[25]; however, rapid Ni deposition has now been found to occur within seconds or minutes[26, 27]. In addition to the amount and acidity of sweat, friction between the skin and metal materials, and the duration and frequency of skin contact, there are several other factors that affect the deposition of Ni on the skin, such as the location of exposure[28, 29], exposure method (occlusive, open, or penetrating exposure)[30], and individual differences in sensitivity[31, 32].

A consensus has been reached that Ni ions released from various alloys penetrate the skin and activate epithelial cells and antigen-presenting cells, such as DCs, which migrate to draining lymph nodes where they present Ni ions to T cells[33]. However, no visual proof that the Ni ions are captured by DCs and transferred to lymph nodes exist. Therefore, in this study, we adapted the use of Newport Green to fluorescently track Ni ions. The complexing agent Newport Green emits fluorescence when combined with Ni is often used to detect Ni in solutions, gels, natural biofilms, and microbial flocs cultivated in laboratories[34-36].

Our experimental results confirmed that free Ni ions could be captured by DCs cultured *in vitro*, reached a peak within 6 h, and were gradually emitted after 24 h. Capturing Ni ions did not affect the activity of DCs. The BMDC image at 1000 × magnification showed double-positive staining particles of Newport Green and MHC II in the cytoplasm, which confirmed that Ni ions were captured and entered DCs. In *in vivo* experiments in of Ni allergy induction in mice, Ni ions entered DCs and showed positive staining in keratinocytes. At the earliest, a small amount of Ni ions was observed in the epidermal sheet within 1 h. After 6 h, the number of Ni ions that entered the epidermal sheet reached a peak and remained constant for a few days. It was not until 48 h later that Ni ions began to be gradually emitted. FACS quantitative analysis of the cervical lymph nodes of mice where Ni allergy was induced showed that the accumulation of Ni ions reached a peak within 24 h, and then gradually decreased. This result confirmed that Ni was indeed captured by epidermal DCs and transferred to lymph nodes (Fig. 7).

It was evident that most of the Newport Green-positive sites were co-localized with the MHC II-positive sites in

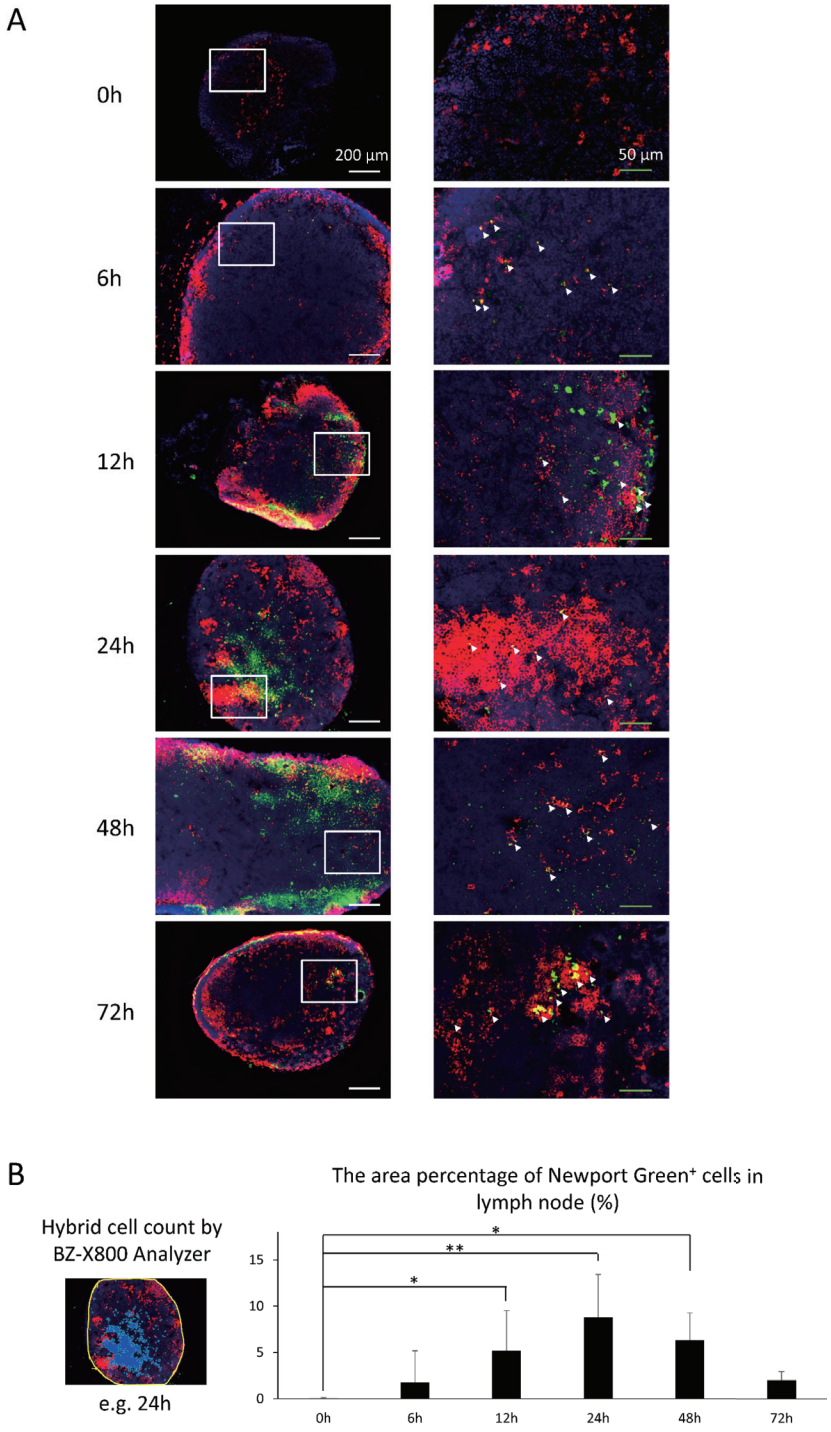

Fig. 5 Immunofluorescence images of of Ni allergy-induced mouse lymph nodes.
(A) Immunofluorescence images of Newport Green and MHC II expression in draining lymph nodes after Ni allergy induction over time. The green represents the Newport Green-positive stain and the red represents the MHC II-positive stain. The yellow (partially indicated by arrow heads) represents the double-positive staining cells. Magnification, × 100 (left), × 400 (right). Scale bar, 200 μm (left), 50 μm (right).
(B) The left panel shows the example of 24 h group image after fluorescence hybrid cell count by BZ-X800 Analyzer software. Inside the yellow line indicates the specified area of lymph node. The blue area indicates the Newport Green-positive area after extraction. The right panel shows the percentage of the Newport Green-positive area in the total area of lymph node after Ni allergy induction over time. Data are shown as mean ± SD of at least 4 images/group. *$p<0.05$, **$p<0.01$, compared to 0 h group. One-Way ANOVA with LSD.

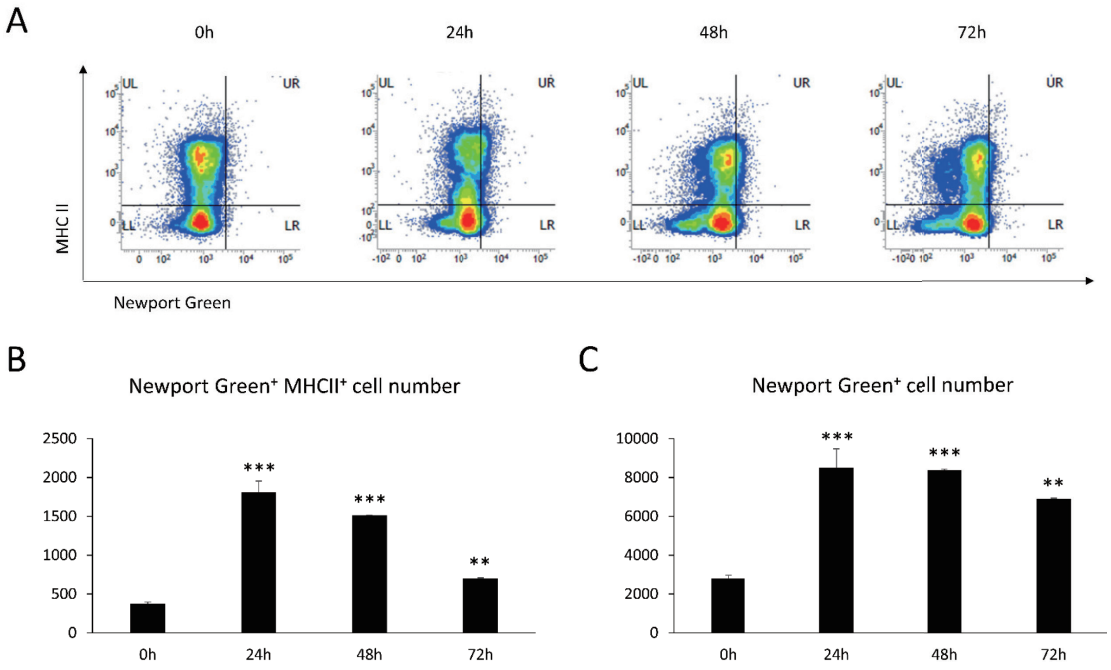

Fig. 6 The FACS analysis of lymph nodes of Ni allergy-induced mice.
(A) The population of Newport Green$^+$ MHC II$^+$ cells in draining lymph nodes from 5 mice/group was analyzed by flow cytometry.
(B and C) The number of Newport Green$^+$ MHC II$^+$ cells and the number of only Newport Green$^+$ cells in the lymph nodes after Ni allergy induction over time are shown. Data are shown as mean ± SD and are representative of four independent experiments. **p<0.01, ***p<0.001. One-Way ANOVA with LSD.

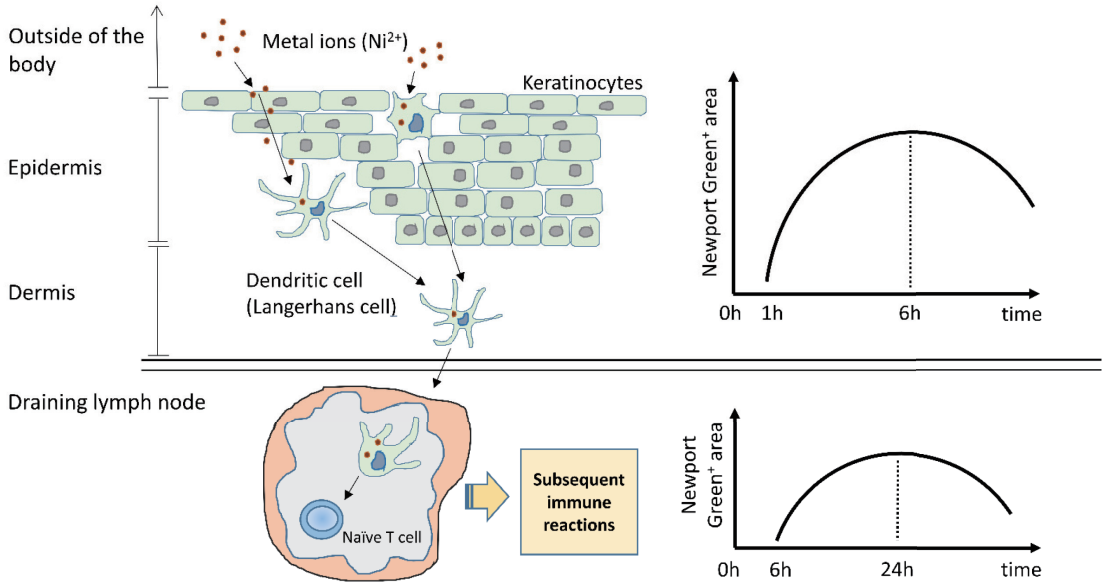

Fig. 7 The hypothetical mechanism diagram of the capture of Ni ions by DCs.
The capture and transportation of metal ions by DCs induce the development of metal allergy. This hypothetical mechanism diagram shows the relationship between the position, number and time of Ni ions in the process of penetrating the skin.

Ni-stimulated BMDCs and in Ni allergy-induced mouse epidermal sheets and lymph nodes. MHC II molecules are found only in professional antigen-presenting cells such as DCs, mononuclear phagocytic cells, endothelial cells, thymic epithelial cells, and B cells[37]. Generally, classical haptens form a stable covalent bond with MHC II-bound proteins, and Ni ions interact with the MHC II molecule and/or the amino acid chain on MHC II bound peptides to form a non-covalent reversible coordination of protein-metal complexes[38]. Some T cells react with this Ni complex on the surface of the MHC/peptide like other haptens; however, in some cases, Ni ions activate T cells by cross-linking receptors with MHC molecules. In addition, the reversible binding of Ni and interacting proteins can mediate the transfer of Ni ions to the receptor-MHC interface[3, 38].

Ni ions were also observed in keratinocytes in the epidermal sheets. Whether they were captured by keratinocytes or just passed through when penetrating the skin remains unclear. In this study, we only studied the relationship between Ni ions and DCs, which is not enough to clarify the complete dynamics of Ni ions penetrating the skin. In future research, we will continue to observe how Ni ions are sensed by keratinocytes, whether keratinocytes also capture and transmit them.

In lymph node sections, we observed Newport Green-positive sites where MHC II staining was negative, indicating that Ni ions can be released in lymph nodes in a free state, or transmitted to other cells. It has been reported that fragments of intracellular metal debris deposited in regional lymph nodes of patients with bone malignancy following insertion of a prosthesis, were found via magnetic resonance imaging[39]. In an autopsy study of subjects using stainless steel and cobalt-chromium alloy prostheses, metals were found in local and distant lymph nodes[40]. This indicates that various metals may be deposited in lymph nodes, and only Newport Green-positive staining may be due to the identification of metals other than Ni deposited in lymph nodes that are present in mouse food or biting a metal cage. Using an indicator that only specifically recognizes Ni may be a better solution to this problem. In our research, Ni ions carried by DCs were observed in the draining lymph nodes. Further studies are required on the possibility that DCs present Ni ions to T cells as antigens and the subsequent kinetics of DCs *in vivo*.

Acknowledgments

This study was supported by the Support Center for Advanced Medical Science, Tokushima University Graduate School of Biomedical Sciences. This work was supported by JSPS KAKENHI Grant Number JP18K09661.

Conflicts of Interest

The authors declare no conflict of interest.

Reference

1）Tramontana M, Bianchi L, Hansel K, Agostinelli D and Stingeni L: Nickel Allergy: Epidemiology, Pathomechanism, Clinical Patterns, Treatment and Prevention Programs. Endocrine, Metabolic & Immune Disorders-Drug Targets (Formerly Current Drug Targets-Immune, Endocrine & Metabolic Disorders) 20, 992-1002 (2020)

2）Martin S F: New concepts in cutaneous allergy. Contact Dermatitis 72, 2-10 (2015)

3）Gamerdinger K, Moulon C, Karp D R, Van Bergen J, Koning F, Wild D, Pflugfelder U and Weltzien H U: A new type of metal recognition by human T cells: contact residues for peptide-independent bridging of T cell receptor and major histocompatibility complex by nickel. The Journal of experimental medicine 197, 1345-1353 (2003)

4）Schmidt M and Goebeler M: Nickel allergies: paying the Toll for innate immunity. Journal of molecular medicine 89, 961 (2011)

5）Cavani A, Nasorri F, Prezzi C, Sebastiani S, Albanesi C and Girolomoni G: Human CD4+ T lymphocytes with remarkable regulatory functions on dendritic cells and nickel-specific Th1 immune responses. Journal of investigative dermatology 114, 295-302 (2000)

6）Rustemeyer T, Von Blomberg B, Van Hoogstraten I, Bruynzeel D and Scheper R: Analysis of effector and regulatory immune reactivity to nickel. Clinical & Experimental Allergy 34, 1458-1466 (2004)

7）Nourshargh S and Alon R: Leukocyte migration into inflamed tissues. Immunity 41, 694-707 (2014)

8）Hirai T, Yoshioka Y, Izumi N, Ichihashi K.i, Handa T, Nishijima N, Uemura E, Sagami K I, Takahashi H, Yamaguchi M and others: Metal nanoparticles in the presence of lipopolysaccharides trigger the onset of metal allergy in mice. Nature nanotechnology 11, 808-816 (2016)

9）Fullerton A, Andersen J R, Hoelgaard A and Menné T: Permeation of nickel salts through human skin in vitro. Contact Dermatitis 15, 173-177 (1986)

10）NEK J J H, Dreher F, Pelosi A, Anigbogu A and Maibach H I: Human stratum corneum penetration by nickel. Acta Derm Venereol 212, 5-10 (2001)

11）Hosty`nek J J, Dreher F, Nakada T, Schwindt D, Anigbogu A and Maibach H I: Human Stratum Corneum Adsorption of Nickel Salts. Acta Dermato-Venereologica 212, 11-18 (2001)

12) Hostynek J J: Sensitization to nickel: etiology, epidemiology, immune reactions, prevention, and therapy. Reviews on environmental health 21, 253-280 (2006)
13) Ross-Hansen K, Østergaard O, Tanassi J T, Thyssen J P, Johansen J D, Menné T and Heegaard N H: Filaggrin is a predominant member of the denaturation-resistant nickel-binding proteome of human epidermis. The Journal of investigative dermatology 134, 1164 (2014)
14) Artik S, von Vultée C, Gleichmann E, Schwarz T and Griem P: Nickel allergy in mice: enhanced sensitization capacity of nickel at higher oxidation states. The Journal of Immunology 163, 1143-1152 (1999)
15) Hostynek J: Factors determining percutaneous metal absorption. Food and Chemical Toxicology 41, 327-345 (2003)
16) FULLERTON A, Andersen J and HOELGAARD A: Permeation of nickel through human skin in vitro–effect of vehicles. British Journal of Dermatology 118, 509-516 (1988)
17) Watanabe M, Ishimaru N, Ashrin M.N, Arakaki R, Yamada A, Ichikawa T and Hayashi Y: A novel DC therapy with manipulation of MKK6 gene on nickel allergy in mice. PloS one 6, e19017 (2011)
18) Ashrin M N, Arakaki R, Yamada A, Kondo T, Kurosawa M, Kudo Y, Watanabe M, Ichikawa T, Hayashi Y and Ishimaru N: A critical role for thymic stromal lymphopoietin in nickel-induced allergy in mice. The Journal of Immunology 192, 4025-4031 (2014)
19) Minami N, Watanabe M, LIU L, Yunizar M F and Ichikawa T: Effect of Semaphorin7A during the Effector Phase of Nickel Allergy. Journal of Oral Health and Biosciences 33, 8-14 (2020)
20) Tschachler E, Schuler G, Hutterer J, Leibl H, Wolff K and Stingl G: Expression of Thy-1 antigen by murine epidermal cells. Journal of investigative dermatology 81, 282-285 (1983)
21) Jameson J, Ugarte K, Chen N, Yachi P, Fuchs E, Boismenu R and Havran W L: A role for skin γδ T cells in wound repair. Science 296, 747-749 (2002)
22) Julander A, Midander K, Herting G, Thyssen J P, White I R, Odnevall Wallinder I and Lidén C: New UK nickel-plated steel coins constitute an increased allergy and eczema risk. Contact Dermatitis 68, 323-330 (2013)
23) Erfani B, Lidén C and Midander K: Short and frequent skin contact with nickel. Contact Dermatitis 73, 222-230 (2015)
24) Fournier P G and Govers T R: Contamination by nickel, copper and zinc during the handling of euro coins. Contact Dermatitis 48, 181-188 (2003)
25) Flint G: A metallurgical approach to metal contact dermatitis. Contact dermatitis 39, 213-221 (1998)
26) Staton I, Ma R, Evans N, Hutchinson R, McLeod C and Gawkrodger D: Dermal nickel exposure associated with coin handling and in various occupational settings: assessment using a newly developed finger immersion method. British Journal of Dermatology 154, 658-664 (2006)
27) Ahlström M.G, Midander K, Menné T, Lidén C, Johansen J D, Julander A and Thyssen J P: Nickel deposition and penetration into the stratum corneum after short metallic nickel contact: An experimental study. Contact dermatitis 80, 86-93 (2019)
28) Johansen J D, Rastogi S, Bruze M, Andersen K E, Frosch P, Dreier B, Lepoittevin J, White I and Menné T: Deodorants: a clinical provocation study in fragrance-sensitive individuals. Contact Dermatitis 39, 161-165 (1998)
29) Magnusson B and Hersle K: Patch test methods. II. Regional variations of patch test responses. Acta dermato-venereologica 45, 257-261 (1965)
30) Fischer L A, Menné T and Johansen J D: Experimental nickel elicitation thresholds -a review focusing on occluded nickel exposure. Contact Dermatitis 52, 57-64 (2005)
31) Friedmann P, Moss C, Shuster S and Simpson J: Quantitative relationships between sensitizing dose of DNCB and reactivity in normal subjects. Clinical and experimental immunology 53, 709 (1983)
32) Johassen J, Andersen K E and Menné T: Quantitative aspects of isoeugenol contact allergy assessed by use and patch tests. Contact Dermatitis 34, 414-418 (1996)
33) Saito M, Arakaki R, Yamada A, Tsunematsu T, Kudo Y and Ishimaru N: Molecular mechanisms of nickel allergy. International journal of molecular sciences 17, 202 (2016)
34) Wuertz S, Müller E, Spaeth R, Pfleiderer P and Flemming H: Detection of heavy metals in bacterial biofilms and microbial flocs with the fluorescent complexing agent Newport Green. Journal of Industrial Microbiology and Biotechnology 24, 116-123 (2000)
35) Costa M, Davidson T L, Chen H, Ke Q, Zhang P, Yan Y, Huang C and Kluz T: Nickel carcinogenesis: epigenetics and hypoxia signaling. Mutation Research/Fundamental and Molecular Mechanisms of Mutagenesis 592, 79-88 (2005)
36) Lawrence J R, Swerhone G D and Neu T R: Visualization of the sorption of nickel within exopolymer microdomains of bacterial microcolonies using confocal and scanning electron microscopy. Microbes and

environments p. ME18134 (2019)
37）Jurewicz M M and Stern L J: Class II MHC antigen processing in immune tolerance and inflammation. Immunogenetics 71, 171-187 (2019)
38）Thierse H J, Gamerdinger K, Junkes C, Guerreiro N and Weltzien H U: T cell receptor (TCR) interaction with haptens: metal ions as non-classical haptens. Toxicology 209, 101-107 (2005)
39）Davies A, Cooper S, Mangham D and Grimer R: Metal-containing lymph nodes following prosthetic replacement of osseous malignancy: potential role of MR imaging in characterisation. European radiology 11, 841-844 (2001)
40）Case C, Langkamer V, James C, Palmer M, Kemp A, Heap P and Solomon L: Widespread dissemination of metal debris from implants. The Journal of bone and joint surgery. British volume 76, 701-712 (1994)

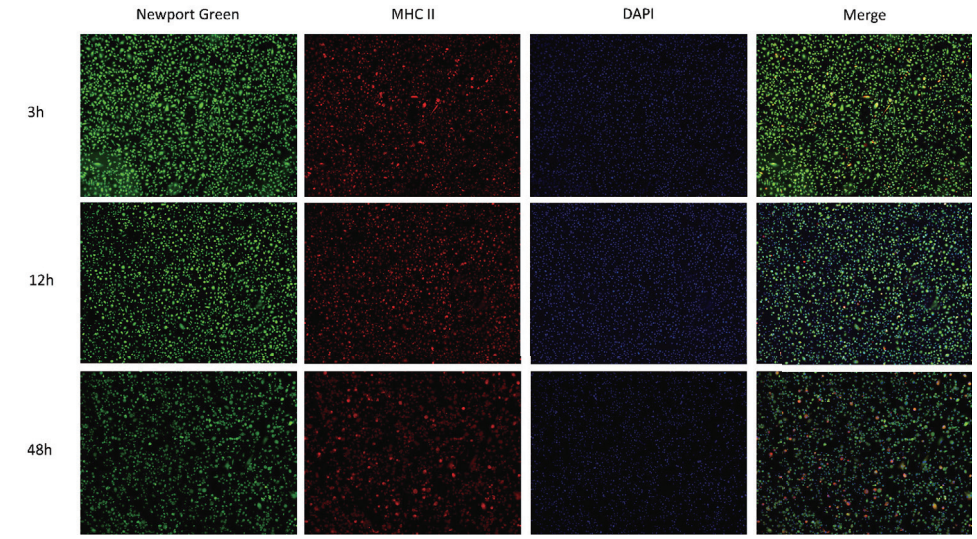

Fig. S1 Newport Green and and MHC II expression in Ni-stimulated BMDCs.
Immunofluorescence images of Newport Green and MHC II expression in cultured BMDCs after 25 μM $NiCl_2$ stimulation over time (3 h, 12 h, 48 h). The yellow color in merged photos represents the DCs that captured Ni ions. Magnification, × 100.

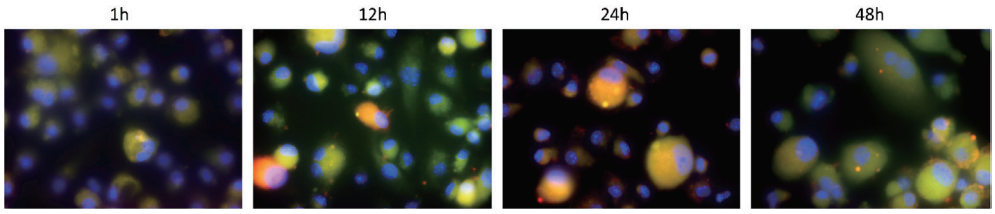

Fig. S2 Newport Green and and MHC II expression in Ni-stimulated BMDCs.
Immunofluorescence images of Newport Green and MHC II expression in cultured BMDCs after 25 μM $NiCl_2$ stimulation over time (1 h, 12 h, 24 h, 48 h). The green represents the Newport Green-positive area, the red represents the MHC II-positive area and the yellow represents the double staining area. Magnification, × 1000.

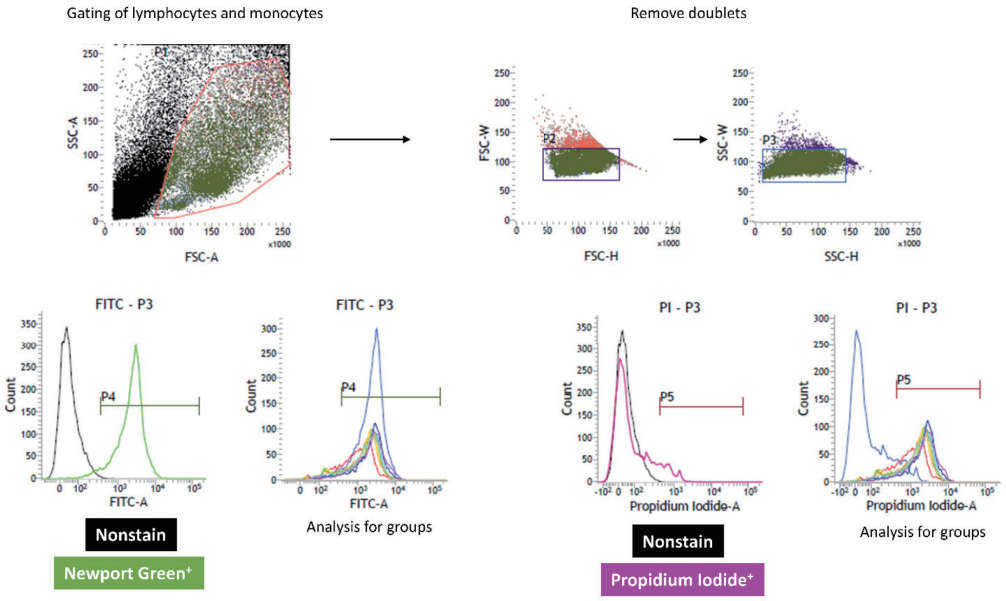

Fig.S3 The flow cytometry gating strategy of BMDCs.
The flow cytometry gating strategy of BMDCs is shown. Forward scatter (FSC) and side scatter (SSC) were used to gate the lymphocytes and monocytes first, after which clumps or doublets were eliminated. By using a negative control and a positive control of Newport Green or Propidium Iodide, the gating of samples was determined.

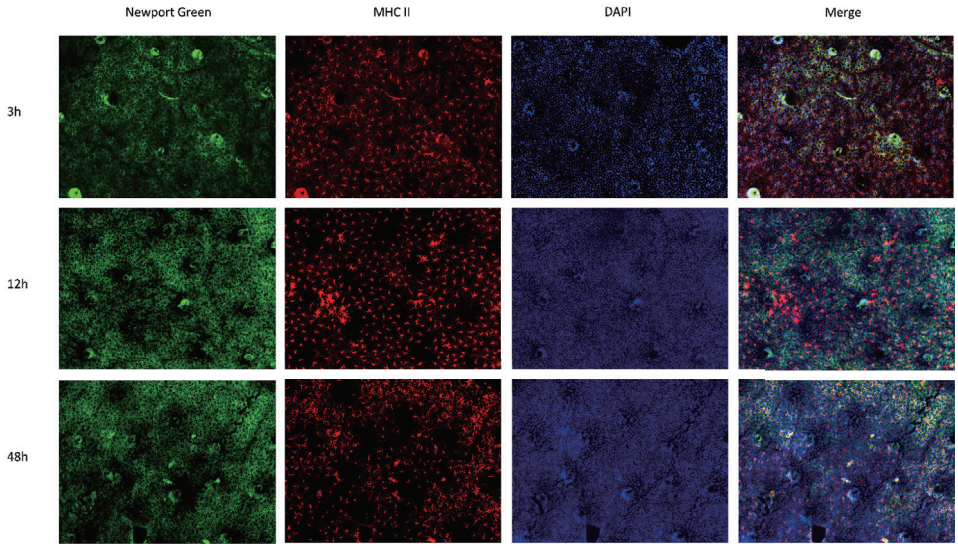

Fig. S4 Immunofluorescence images of Newport Green and MHC II expression in Ni allergy-induced mouse epidermal sheets.
Immunofluorescence images of Newport Green and MHC II expression in epidermal sheets after Ni allergy induction over time (3 h, 12 h, 48 h). The yellow color in merged photos represents the DCs that captured Ni ions. Magnification, × 200.

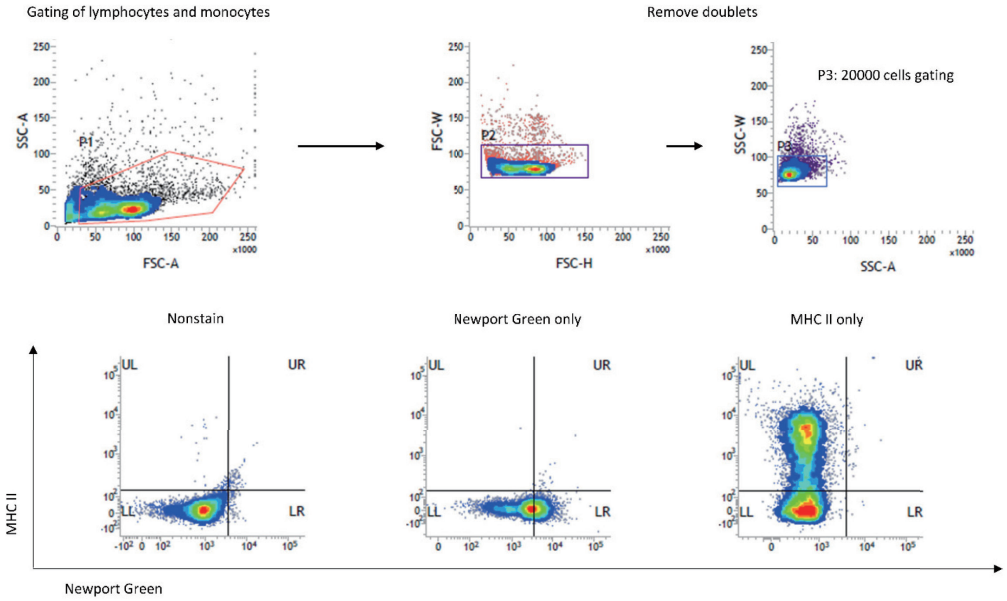

Fig. S5 The flow cytometry gating strategy of lymph node single cell suspensions.
The flow cytometry gating strategy of lymph node single cell suspensions is shown. FSC and SSC were used to gate the lymphocytes and monocytes first, after which clumps or doublets were eliminated. By using a negative control and a positive control of Newport Green or MHC II, the gating of samples was determined.